Multistability of Driven-Dissipative Quantum Spins

Haggai Landa,[1,*] Marco Schiró,[2,†] and Grégoire Misguich[1,3,‡]
[1]Institut de Physique Théorique, Université Paris-Saclay, CEA, CNRS, 91191 Gif-sur-Yvette, France
[2]JEIP, USR 3573 CNRS, Collège de France, PSL Research University,
11, place Marcelin Berthelot, 75231 Paris Cedex 05, France
[3]Laboratoire de Physique Théorique et Modélisation, CNRS UMR 8089, Université de Cergy-Pontoise,
95302 Cergy-Pontoise, France

(Received 30 May 2019; published 29 January 2020)

We study the dynamics of lattice models of quantum spins one-half, driven by a coherent drive and subject to dissipation. Generically the mean-field limit of these models manifests multistable parameter regions of coexisting steady states with different magnetizations. We introduce an efficient scheme accounting for the corrections to mean field by correlations at leading order, and benchmark this scheme using high-precision numerics based on matrix-product operators in one- and two-dimensional lattices. Correlations are shown to wash the mean-field bistability in dimension one, leading to a unique steady state. In dimension two and higher, we find that multistability is again possible, provided the thermodynamic limit of an infinitely large lattice is taken *first* with respect to the longtime limit. Variation of the system parameters results in jumps between the different steady states, each showing a critical slowing down in the convergence of perturbations towards the steady state. Experiments with trapped ions can realize the model and possibly answer open questions in the nonequilibrium many-body dynamics of these quantum systems, beyond the system sizes accessible to present numerics.

DOI: 10.1103/PhysRevLett.124.043601

Coherent control over quantum single- and few-body dynamics is continuously improving, spanning atomic, optical, and solid-state systems [1–3]. An ongoing effort is focused on assembling many individually tunable systems and studying the ensuing many-body dynamics. A significant challenge lies in realizing unitary dynamics, however, the inevitable presence of dissipative processes can be utilized in different scenarios, such as by reservoir engineering [4]. Coherent time-periodic driving is a useful tool [5], and rich dynamics are observed with systems of strong light-matter interactions at the interface between quantum optics and condensed matter [6–22]. Systems with a competition between interactions, nonlinearity, coherent external driving and dissipative dynamics include arrays of coupled circuit quantum electrodynamic units [23,24], cold atoms [25], and ions [26]. Critical phenomena and dissipative phase transitions in these open systems often come with new properties and novel dynamic universality classes [27–32].

The state of an open quantum system is defined by a density matrix ρ, with the dynamics often treated using a Lindblad master equation, describing a memoryless bath, and the time evolution generated by the Liouvillian superoperator acting on ρ [33]. The theoretical tools available for open quantum many-body systems are relatively limited. For driven-dissipative lattice models the mean-field (MF) approach is often employed, with ρ approximated as a product of single-site density matrices. The dynamics of local observables are described by nonlinear equations, studied, e.g., for lattice Rydberg atoms [34–39], coupled quantum-electrodynamics cavities and circuits [20,40,41], nonlinear photonic models [42,43], and spin lattices [44,45]. A key feature of the MF phase diagrams are multistable parameter regions where two or more steady states coexist.

However, the Lindblad equation converges in general to a unique steady state in finite systems [46,47], making the status of the MF approximation unclear. Indeed, significant deviations from MF have been found using approximation schemes accounting for quantum correlations [48–50], and also using exact numerical methods (quantum trajectories [51] and matrix product operators (MPO) [52]). In one-dimensional (1D) lattices with nearest-neighbor (NN) interactions, the MF bistability is found to be replaced by a crossover driven by large quantum fluctuations [42,48,53,54]. In contrast, in certain 2D NN models, MF bistability has been found by approximate methods to be replaced by a first-order phase transition between two states, for nonlinear bosons using a truncated Wigner approximation [42,54], and for Ising spins using a variational ansatz accounting for short-range correlations [48], a cluster MF approach [55], and two-dimensional tensor network states [56]. In a parameter region around the jump, the convergence towards the steady state slows down [48,54], a phenomenon related to a gap closing in the spectrum of the Liouvillian [47,57,58].

In this Letter, we study a driven-dissipative model of spins one-half with XY (flip-flop) interactions in the presence of coherent drive and dissipation, using a combination of MPO simulations and an approximation scheme which accounts for quantum fluctuations beyond mean field (MFQF). For one-dimensional lattices we confirm the existence of a unique steady state in the thermodynamic limit. As our main result, we find that in dimension two and higher multistability (in particular, bistability) is again possible, with jumps between the different steady states accompanied by a critical slowing down, provided that the thermodynamic limit of an infinitely large lattice is taken *first* with respect to the longtime limit. We argue that this order of limits is physically plausible, and we link the bistability to the fact that for finite size and time the probability distribution of relevant observables develops a strong bimodal structure. Depending on the order of limits, bimodality leads either to a first-order dissipative phase transition (as usually discussed when the longtime limit is taken first), or to a bistable regime. We thus provide a theoretical scenario reconciling our results with the literature cited above, and finding similar dynamics in a model with Ising interactions (see below and [59]) indicates the generality of our results. We suggest that in an experimental platform based on trapped-ion quantum simulators, such a question can be addressed.

Model.—We consider a quantum system with N sites $R \in \mathbb{Z}^D$ on a hypercubic lattice in D spatial dimensions, for which the connectivity is $\mathcal{Z} = 2D$. The master equation for ρ is defined using the Liouvillian $\hat{\mathcal{L}}$,

$$\partial_t \rho = \hat{\mathcal{L}}[\rho] \equiv -i[H,\rho] + \mathcal{D}[\rho], \qquad \hbar = 1. \tag{1}$$

The Hamiltonian describing Rabi oscillations of two-level systems with a drive detuned by Δ from the resonant transition frequency and a Rabi frequency Ω, is given in a frame rotating with the drive by

$$H = \sum_R \left[\frac{\Delta}{2}\sigma_R^z + \Omega\sigma_R^x\right] - \sum_{\langle R,R'\rangle} J(\sigma_R^+\sigma_{R'}^- + \text{H.c.}), \tag{2}$$

where the second sum extends over all pairs of NN sites, describing hopping with amplitude J, with spin-$\frac{1}{2}$ operators (Pauli matrices) σ_R^a, $a = \{x,y,z\}$, and $\sigma_R^\pm = (\sigma_R^x \pm i\sigma_R^y)/2$. For spin losses occurring independently at each site with rate $\Gamma = 1$ (which fixes the frequency and time units),

$$\mathcal{D}[\rho] = \sum_R \left[\sigma_R^-\rho\sigma_R^+ - \frac{1}{2}(\sigma_R^+\sigma_R^-\rho + \rho\sigma_R^+\sigma_R^-)\right]. \tag{3}$$

Aside from translation invariance, this model has no manifest microscopic symmetries. Its MF phase diagram displays bistability [45,53] in a region of parameters that terminates at a second order point where an emerging Z_2 symmetry spontaneously breaks [36]. In 1D the steady state is unique as obtained by MPO simulations [53]. Here we focus on higher dimensions, which we find to manifest bistability in the thermodynamic limit.

Dynamics of observables.—From the master equation one can derive a hierarchy of equations of motion for n-point expectation values of the form $\langle\sigma_{R_1}^a\sigma_{R_2}^b\cdots\sigma_{R_n}^c\rangle \equiv \text{tr}\{\rho\sigma_{R_1}^a\sigma_{R_2}^b\cdots\sigma_{R_n}^c\}$, which depend on the value of correlators at the next order, $n+1$. Assuming a translationally invariant density matrix, we define the uniform vector mean magnetization, $\mu_a(t) = \langle(1/N)\sum_R \sigma_R^a\rangle = \langle\sigma_R^a\rangle$, and its equations of motion

$$\partial_t\mu_x = -J\mathcal{Z}[\mu_y\mu_z + \eta_{yz}(1)] - \Delta\mu_y - \mu_x/2, \tag{4}$$

$$\partial_t\mu_y = J\mathcal{Z}[\mu_x\mu_z + \eta_{xz}(1)] - 2\Omega\mu_z + \Delta\mu_x - \mu_y/2, \tag{5}$$

$$\partial_t\mu_z = 2\Omega\mu_y - (1+\mu_z). \tag{6}$$

with the connected two-point correlation functions,

$$\begin{aligned}\eta_{ab}(R,R',t) &\equiv \langle(\sigma_R^a - \mu_a)(\sigma_{R'}^b - \mu_b)\rangle \\ &= \langle\sigma_R^a\sigma_{R'}^b\rangle - \mu_a\mu_b, \qquad R \neq R',\end{aligned} \tag{7}$$

and setting $R' = 0$ using the translation invariance, $\eta_{ab}(1)$ is the correlator at a NN of the origin.

Equations (4)–(6) are exact. The limit $\eta \to 0$ reduces ρ to a product of identical on-site states, leading to the MF equations, whose steady state and dynamics are studied in detail in [60]. We present an approximate scheme going beyond MF, formally based on an expansion in $1/\mathcal{Z}$ (with a related approach in [49]). Neglecting the connected three-point correlators $\langle(\sigma_R^a-\mu_a)(\sigma_{R'}^b-\mu_b)(\sigma_{R''}^c-\mu_c)\rangle \approx 0$, allows us to derive (see [59]) coupled equations for $\eta_{ab}(R,t)$, which we solve numerically together with their feedback into Eqs. (4)–(6). Since the short-range correlators $\eta_{ab}(1)$ appearing in Eqs. (4)–(6) are dynamically coupled to all distances in the lattice, the MFQF method accounts for the spatial structure of correlation functions. The simulations have been verified to converge as a function of N, and hence we can approximate the system dynamics as a function of time with the limit $N \to \infty$ taken first.

Correlations wash away bistability in 1D.—We start our analysis with numerically exact MPO calculations of large lattices in 1D. The density matrix ρ can be considered as a pure state in an enlarged Hilbert space with four states per site [61], allowing us to solve the Lindblad evolution using a method formally similar to pure state unitary evolution encoded using well-established matrix product states (see [62,63], and references therein). We evolve $\rho(t)$ in a 1D chain with open boundary conditions (translation invariance is not enforced), using an MPO algorithm [52,61,64], with an implementation based on the iTensor library [65], a Trotter decomposition of order four [63,66], and bond dimension $\chi = 300$. With up to 200 spins we

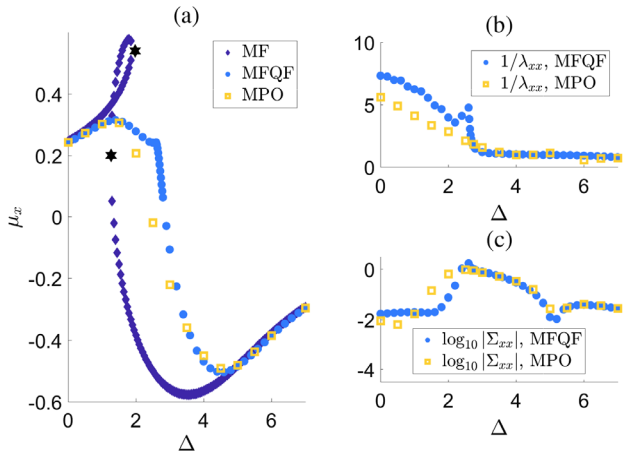

FIG. 1. (a) Mean steady-state x magnetization μ_x^S as a function of Δ for $\Omega = 0.5$ and $J\mathcal{Z} = 4$, on a 1D lattice. The mean-field (MF) limit manifests bistability, with three coexisting solutions, two of which—those on the branches coming from the limits of $\Delta \to \{0, \infty\}$, are stable. Two black hexagrams mark the points where the unstable branch meets each of the two stable ones. An exact numerical treatment using matrix product operators (MPO) shows a crossover within a range of Δ shifted from the MF bistability region. An approximation incorporating quantum fluctuations at leading order (MFQF) follows approximately the MPO result in a large range of parameters. (b) The correlation length λ_{xx} defined by fitting $\eta_{xx} \sim \exp\{-\lambda_{xx}R\}$, and (c) the total correlation $\Sigma_{xx} = \sum_R \eta_{xx}(R)$, calculated in MPO and MFQF, showing that the latter approximation is capable of capturing the spatial structure and relative magnitudes of two-point correlations in the lattice.

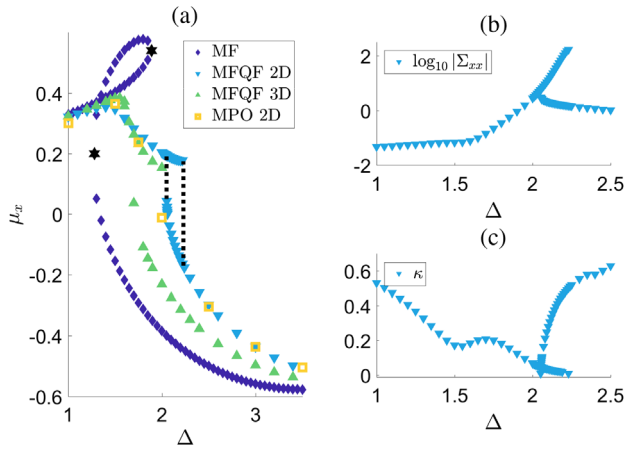

FIG. 2. (a) Mean steady-state x magnetization μ_x^S in the MFQF $N \to \infty$ approximation in 2D–3D, together with the MF limit and 2D-MPO results (for a 12×4 cylinder). The parameters are as in Fig. 1, with $J\mathcal{Z}$ kept fixed by varying J with the dimension. For $D \geq 2$ MFQF predicts multistability, with two stable branches approaching the MF branches in an increasingly larger parameter region as D is increased. The dotted black lines indicate the edges of the 2D bistable region. The simulations were run with lattices of up to 200^2 and 40^3 sites and periodic boundary conditions. (b) The total correlation in 2D, showing a difference of up to 2 orders of magnitude in the bistable phases. (c) The rate of convergence to the 2D steady states, fitted to an exponential form $\sim e^{-\kappa t}$, showing a critical slowing down of the dynamics as $\kappa \to 0$ at the two bistability edges.

checked that observables measured in the central region of the chain had negligible finite-size effects and truncation errors at the scale of the plots, allowing us to obtain their steady-state bulk values corresponding to the thermodynamic limit.

Figure 1(a) shows the x component of the steady-state magnetization, $\vec{\mu}^S \equiv \lim_{t\to\infty}\vec{\mu}(t)$, in 1D, for $J\mathcal{Z} = 4$ as a function of Δ. In MF, $\vec{\mu}^S$ is unique except for $1.3 \lesssim \Delta \lesssim 1.9$, where there are two coexisting stable solutions in addition to an unstable solution. At the presence of quantum correlations (in MPO and MFQF), the magnetization departs significantly from the MF prediction, with a crossover between the two limiting regimes, in the range $1.5 \lesssim \Delta \lesssim 5$. We define the inverse correlation lengths λ_{ab} by fitting the six correlation functions to $\eta_{ab}(R) \sim \exp\{-\lambda_{ab}R\}$. For simplicity, we present in Fig. 1(b) only one correlation length, and Fig. 1(c) shows the corresponding total correlation measured by $\Sigma_{ab} = \sum_R \eta_{ab}(R)$. The spatial structure of the two-point correlation undergoes a sharp change within the crossover region, from relatively small but widely extended correlations for low Δ, to much larger but very short-ranged correlations, for high Δ. A separate analysis of the correlations shows that at the same time, the correlations change nature from periodic modulations (spin density-wave character), to being overdamped in space.

As Fig. 1 shows, the MFQF approximation correctly captures the uniqueness of the steady state and the disappearance of bistability in 1D. On both sides of the crossover region, the results are quantitatively accurate. In its center, the approximation reaches too large values for $\eta_{ab}(R)$ and the correlation length. More generally, we find that as J is increased in 1D, the MFQF approach loses its accuracy (for parameters of strong correlations), plausibly because of the role of higher-order correlation functions that are neglected, which can lead at much larger J to the breakdown of the approximation. However, the MFQF approach is easy to generalize to higher dimensions, and quantitatively accurate in regions with moderate correlations.

Bistability in higher dimensions.—Figure 2(a) shows the results of simulations with large 2D and 3D lattices, for $J\mathcal{Z} = 4$. The MFQF theory, that allows simulating large lattices (with $N \to \infty$), is compared with 2D-MPO calculations, limited to a finite-size system, for which, as in 1D, ρ is encoded as a product of matrices. The matrix product runs over a snakelike path visiting all the sites of a cylinder of length $L_x = 12$ and perimeter $L_y = 4$ (see [59]). Such an approach has been applied in ground-state calculations of 2D models [67], but we are not aware of previous 2D-MPO Lindblad calculations. For $\Delta \lesssim 1.5$ and $\Delta \gtrsim 2.5$ the agreement between MPO and MFQF is almost perfect, giving a nontrivial check of the ability of MFQF to capture significant correlation effects (that result in $\vec{\mu}$ strongly

departing from MF). The computational cost of guaranteeing a high accuracy in 2D-MPO calculation is exponential in L_y (see [59]), limiting the present MPO calculations to relatively small systems, which cannot show bistability (and a possible discontinuity would also be smeared out).

As our main result, using MFQF we find in 2D two stable $\vec{\mu}^S$ branches, that in 3D extend over larger ranges of Δ, converging towards the MF bistability region and magnetization values. Figure 2(b) shows that Σ_{xx} increases by 2 orders of magnitude for one of the bistable states, and Fig. 2(c) shows the asymptotic relaxation rate associated with the convergence to $\vec{\mu}^S$. It is obtained by fitting $\partial_t \vec{\mu}^2 \sim e^{-\kappa t}$ at large times ($t \sim 100$). The fact that $\kappa \to 0$ at the branch edges in 2D indicates a critical slowing down when approaching the end of the bistability region in the phase that is about to disappear, leading to a discontinuous jump. The MFQF approach does, however, not *always* predict bistability in 2D. Replacing each hopping term in Eq. (2) by the Ising coupling $J_z \sigma^z_R \sigma^z_{R'}$, we find a smooth crossover for moderate J_z (as obtained using cluster mean field [55]), and a small bistability region for stronger couplings (again as in [55]); see [59].

Bistability, Liouvillian spectrum and bimodality.—We henceforth return to the question raised in the introduction: how to reconcile the uniqueness of the steady state in finite systems, with bistability seen when taking first the thermodynamic limit of infinite size, and then the long-time limit?

Considering the Liouvillian $\hat{\mathcal{L}}$ of Eq. (1), the unique thermodynamic steady state corresponds to $\rho_{ss} = \lim_{N\to\infty} \lim_{t\to\infty} \rho(t)$, which is independent of the initial conditions, and is an eigenstate of $\hat{\mathcal{L}}$ at any N, $\hat{\mathcal{L}}\rho_{ss} = 0$. Assuming bistability, we define ρ_1 and ρ_2 as the two distinct density matrices obtained from $\lim_{t\to\infty} \lim_{N\to\infty} \rho(t)$, which depend on the initial conditions. For N large but finite the bistability should be replaced by long-lived metastable states, in which case ρ_1 and ρ_2 are defined at times $t \gg 1/\Gamma$, but small compared to the lifetime of these metastable states. As in the model studied here, these two states have different local properties: a local observable [i.e., sum of local terms, e.g., $M_x = (1/N)\sum_R \sigma^x_R$] has a probability distribution $P_1(m)$ with a single peak centred around m_1 in ρ_1, and a distribution $P_2(m)$ peaked around m_2 ($\neq m_1$) in ρ_2. At the same time, metastability implies some relaxation time diverging with N, and the spectrum of $\hat{\mathcal{L}}$ must have at least one nonzero eigenvalue λ_E with a vanishingly small real part, $\lim_{N\to\infty} \mathrm{Re}(\lambda_E) = 0$, other eigenvalues being separated by a gap $\mathcal{O}(\Gamma)$ [58,68]. We assume for simplicity that $\hat{\mathcal{L}}$ has a unique such small eigenvalue (therefore real), and denote by ρ_E the associated eigenstate (or eigenmatrix). ρ_{ss} and ρ_E are the eigenstates from which all long-lived states can be constructed, since for t much larger than $1/\Gamma$ we can ignore higher "excited" eigenstates. So, for ρ_1 and ρ_2 to be long lived, they must be linear combinations of ρ_{ss} and ρ_E. As physical states have a trace equal to 1, and since $\mathrm{Tr}\rho_{ss} = 1$ and $\mathrm{Tr}\rho_E = 0$, there must exist two distinct scalars a_1 and a_2 such that $\rho_i = \rho_{ss} + a_i \rho_E$ with $i = 1, 2$ [38,47,58,68]. Inverting these relations we get $\rho_{ss} = (a_2\rho_1 - a_1\rho_2)/(a_2 - a_1)$. So, if a_1 and a_2 are both nonzero (which may not be always the case) ρ_{ss} is a "cat state" (with correlation functions extending over the system size), being a linear combination of two uniform physical states with different local properties. In ρ_{ss}, the probability distribution $P_{ss} = (a_2 P_1 - a_1 P_2)/(a_2 - a_1)$ of a local observable is *bimodal*, peaked around the two mean values $m_{1,2}$ realized in the states $\rho_{i=1,2}$.

Using exact diagonalization on small systems we have computed such distributions for the fully connected version of the present XY model, which is bistable in the thermodynamic limit (where MF becomes exact), and for the 1D and 2D cases. We find ([59]), that the magnetization becomes bimodal in parts of the MF bistability region for the fully connected and 2D cases, whereas it stays monomodal in 1D. The scaling with N of the bimodal peaks is beyond the scope of the current work, however, the mean value of an observable computed with ρ_{ss} may become *discontinuous* as $N \to \infty$ at some value of the parameter [42,47,54,69]. This could correspond, in the discussion above, to smoothly varying $\rho_{i=1,2}$ but discontinuous jumps of a_1 and a_2. Hence, a unique steady state with a discontinuous jump is *a priori* compatible with bistability and hysteresis and, in the present scenario, finding one or the other in a theory calculation is a matter of order of limits.

Moreover, since the support of P_1 has essentially no overlap with that of P_2 (for a large enough system), any density matrix which is not a convex combination of ρ_1 and ρ_2 would give some (unphysical) negative probability density. This means that all physical long-lived states are convex combinations of the monomodal states ρ_i, and the latter thus coincide with the extreme states of [58]. The above discussion therefore connects our results both with the theories of first-order phase transitions, and the theory based on the extreme metastable states. The lifetimes of the many-body metastable states would diverge with N, plausibly $\propto e^N$, and for large enough N, exceed the time accessible in numerical or experimental realizations. We conjecture that an initial state with a finite correlation length will lead, in the time window $1/\Gamma \ll t \ll 1/|\lambda_E|$, to one of the two monomodal states ρ_i, and *not* to an arbitrary combination of the two. A heuristic argument is given in [59]. A product state is a natural reproducible initial state in an experiment, allowing to explore the metastability. As a parameter is swept back and forth across the bistability region in an experimental setup, observables will show hysteresis loops—unless the sweep is unrealistically slow ($\propto e^{-N}$).

Experimental feasibility.—In addition to possible realizations with circuit-QED arrays [53], driven-dissipative spin models can be realized in current experiments with a few tens to a few hundreds of trapped ions. Ising and XY interactions can be implemented by laser beams inducing spin-motion coupling along one or two orthogonal

directions [70–72], with an additional laser for the on-site Hamiltonian. As recently demonstrated experimentally, the interaction can be varied from being almost independent of distance to a dipolar power law, and therefore short range in 1D [73,74] and 2D lattices [26]. The interaction strength in these works is of the order of $J/\hbar \sim 10^4$ s^{-1}, 1 to 2 orders of magnitude larger than the qubit dephasing rates, and the rate of spin-flip processes in Eq. (3) can be potentially controlled as well.

Conclusion.—Studying lattices of driven-dissipative interacting spins using state-of-the-art 1D MPO simulations, for the parameters presented here and in further parameter regimes [60], we have found no phase transition but a crossover between two regimes with different characteristics. On the other hand, using a new approach that accounts for the leading-order lattice correlations and their feedback onto the mean magnetization, bistability appears to be possible in driven-dissipative quantum systems already in 2D. Thus, the present exact and approximate calculations suggest that $D = 2$ is a lower critical dimension for bistability in this problem. This conclusion is consistent with works done in the context of Rydberg atoms on related models [36], pointing toward a model A dynamic universality class (whose lower critical dimension is known to be two) for the second order phase transition at the ending point of the bistability regime. This implies that in one dimension fluctuations destroy the critical point and with it the entire bistability region, in line with our results.

The question of the existence of a lower critical dimension for bistability, bimodality, and hysteresis and the accompanied dissipative phase transitions in this model can be directly addressed experimentally. If a definite answer is found, it would constitute the first demonstration of deciding a question currently intractable classically, by a controlled quantum simulation. It could ascertain the status of the mean-field approximation in these systems, and shed light on the differences between equilibrium and nonequilibrium phase transitions.

We acknowledge the Directrion de la Recherche Fondamentale of CEA for providing us with computer time on the supercomputer COBALT of the Centre de Calcul Recherche et Technologie. H. L. thanks Roni Geffen for fruitful discussions, and acknowledges support by initiative de Recherche Stratégique Ingénierie Quantique à l'Université Paris-Saclay of Université Paris-Saclay and by LabEx Physique Atomes Lumière Matière under Grant No. ANR-10-LABX-0039-PALM.

*haggaila@gmail.com
†marco.schiro@ipht.fr
On Leave from Institut de Physique Théorique, Université Paris Saclay, CNRS, CEA, F-91191 Gif-sur-Yvette, France.
‡gregoire.misguich@cea.fr

[1] S. Haroche and J. Raimond, *Exploring the Quantum: Atoms, Cavities, and Photons*, 1st ed. (Oxford University Press, Oxford, 2006).
[2] Y. Yamamoto, F. Tassone, and H. Cao, *Semiconductor Cavity Quantum Electrodynamics*, 1st ed. (Springer, New York, 2000).
[3] R. J. Schoelkopf and S. M. Girvin, Wiring up quantum systems, Nature (London) **451**, 664 (2008).
[4] C.-E. Bardyn, M. A. Baranov, C. V. Kraus, E. Rico, A. Imamoğlu, P. Zoller, and S. Diehl, Topology by dissipation, New J. Phys. **15**, 085001 (2013).
[5] T. Oka and S. Kitamura, Floquet engineering of quantum materials, Annu. Rev. Condens. Matter Phys. **10**, 387 (2019).
[6] A. D. Greentree, C. Tahan, J. H. Cole, and L. C. L. Hollenberg, Quantum phase transitions of light, Nat. Phys. **2**, 856 (2006).
[7] M. J. Hartmann, F. G. S. L. Brandão, and M. B. Plenio, Strongly interacting polaritons in coupled arrays of cavities, Nat. Phys. **2**, 849 (2006).
[8] D. E. Chang, V. Gritsev, G. Morigi, V. Vuletić, M. D. Lukin, and E. A. Demler, Crystallization of strongly interacting photons in a nonlinear optical fibre, Nat. Phys. **4**, 884 (2008).
[9] J. Koch, A. A. Houck, K. L. Hur, and S. M. Girvin, Time-reversal-symmetry breaking in circuit-QED-based photon lattices, Phys. Rev. A **82**, 043811 (2010).
[10] A. Petrescu, A. A. Houck, and K. Le Hur, Anomalous Hall effects of light and chiral edge modes on the Kagomé lattice, Phys. Rev. A **86**, 053804 (2012).
[11] J. Cho, D. G. Angelakis, and S. Bose, Fractional Quantum Hall State in Coupled Cavities, Phys. Rev. Lett. **101**, 246809 (2008).
[12] R. O. Umucalılar and I. Carusotto, Artificial gauge field for photons in coupled cavity arrays, Phys. Rev. A **84**, 043804 (2011).
[13] M. Hafezi, M. D. Lukin, and J. M. Taylor, Non-equilibrium fractional quantum Hall state of light, New J. Phys. **15**, 063001 (2013).
[14] M. C. Rechtsman, J. M. Zeuner, Y. Plotnik, Y. Lumer, D. Podolsky, F. Dreisow, S. Nolte, M. Segev, and A. Szameit, Photonic Floquet topological insulators, Nature (London) **496**, 196 (2013).
[15] J. Otterbach, M. Moos, D. Muth, and M. Fleischhauer, Wigner Crystallization of Single Photons in Cold Rydberg Ensembles, Phys. Rev. Lett. **111**, 113001 (2013).
[16] I. Carusotto and C. Ciuti, Quantum fluids of light, Rev. Mod. Phys. **85**, 299 (2013).
[17] K. Le Hur, L. Henriet, A. Petrescu, K. Plekhanov, G. Roux, and M. Schiró, Many-body quantum electrodynamics networks: Non-equilibrium condensed matter physics with light, C.R. Phys. **17**, 808 (2016).
[18] C. Noh and D. G. Angelakis, Quantum simulations and many-body physics with light, Rep. Prog. Phys. **80**, 016401 (2017).
[19] M. J. Hartmann, Quantum simulation with interacting photons, J. Opt. **18**, 104005 (2016).
[20] M. Schiró, C. Joshi, M. Bordyuh, R. Fazio, J. Keeling, and H. Türeci, Exotic Attractors of the Nonequilibrium Rabi-Hubbard Model, Phys. Rev. Lett. **116**, 143603 (2016).

[21] M. Fitzpatrick, N. M. Sundaresan, A. C. Y. Li, J. Koch, and A. A. Houck, Observation of a Dissipative Phase Transition in a One-Dimensional Circuit QED Lattice, Phys. Rev. X **7**, 011016 (2017).
[22] J. M. Fink, A. Dombi, A. Vukics, A. Wallraff, and P. Domokos, Observation of the Photon-Blockade Breakdown Phase Transition, Phys. Rev. X **7**, 011012 (2017).
[23] A. A. Houck, H. E. Türeci, and J. Koch, On-chip quantum simulation with superconducting circuits, Nat. Phys. **8**, 292 (2012).
[24] S. Schmidt and J. Koch, Circuit QED lattices: Towards quantum simulation with superconducting circuits, Ann. Phys. (Amsterdam) **525**, 395 (2013).
[25] I. Bloch, J. Dalibard, and S. Nascimbène, Quantum simulations with ultracold quantum gases, Nat. Phys. **8**, 267 (2012).
[26] J. G. Bohnet, B. C. Sawyer, J. W. Britton, M. L. Wall, A. M. Rey, M. Foss-Feig, and J. J. Bollinger, Quantum spin dynamics and entanglement generation with hundreds of trapped ions, Science **352**, 1297 (2016).
[27] S. Diehl, A. Tomadin, A. Micheli, R. Fazio, and P. Zoller, Dynamical Phase Transitions and Instabilities in Open Atomic Many-Body Systems, Phys. Rev. Lett. **105**, 015702 (2010).
[28] L. M. Sieberer, S. D. Huber, E. Altman, and S. Diehl, Dynamical Critical Phenomena in Driven-Dissipative Systems, Phys. Rev. Lett. **110**, 195301 (2013).
[29] T. E. Lee, S. Gopalakrishnan, and M. D. Lukin, Unconventional Magnetism via Optical Pumping of Interacting Spin Systems, Phys. Rev. Lett. **110**, 257204 (2013).
[30] J. Jin, D. Rossini, R. Fazio, M. Leib, and M. J. Hartmann, Photon Solid Phases in Driven Arrays of Nonlinearly Coupled Cavities, Phys. Rev. Lett. **110**, 163605 (2013).
[31] J. Marino and S. Diehl, Driven Markovian Quantum Criticality, Phys. Rev. Lett. **116**, 070407 (2016).
[32] O. Scarlatella, R. Fazio, and M. Schiró, Emergent finite frequency criticality of driven-dissipative correlated lattice bosons, Phys. Rev. B **99**, 064511 (2019).
[33] H.-P. Breuer and F. Petruccione, *The Theory of Open Quantum Systems*, 1st ed. (Oxford University Press, New York, 2002).
[34] T. E. Lee, H. Häffner, and M. C. Cross, Antiferromagnetic phase transition in a nonequilibrium lattice of Rydberg atoms, Phys. Rev. A **84**, 031402(R) (2011).
[35] J. Qian, G. Dong, L. Zhou, and W. Zhang, Phase diagram of Rydberg atoms in a nonequilibrium optical lattice, Phys. Rev. A **85**, 065401 (2012).
[36] M. Marcuzzi, E. Levi, S. Diehl, J. P. Garrahan, and I. Lesanovsky, Universal Nonequilibrium Properties of Dissipative Rydberg Gases, Phys. Rev. Lett. **113**, 210401 (2014).
[37] C. Carr, R. Ritter, C. G. Wade, C. S. Adams, and K. J. Weatherill, Nonequilibrium Phase Transition in a Dilute Rydberg Ensemble, Phys. Rev. Lett. **111**, 113901 (2013).
[38] F. Letscher, O. Thomas, T. Niederprüm, M. Fleischhauer, and H. Ott, Bistability versus Metastability in Driven Dissipative Rydberg Gases, Phys. Rev. X **7**, 021020 (2017).
[39] C. D. Parmee and N. R. Cooper, Phases of driven two-level systems with nonlocal dissipation, Phys. Rev. A **97**, 053616 (2018).
[40] J. Jin, D. Rossini, R. Fazio, M. Leib, and M. J. Hartmann, Photon Solid Phases in Driven Arrays of Nonlinearly Coupled Cavities, Phys. Rev. Lett. **110**, 163605 (2013).
[41] J. Jin, D. Rossini, M. Leib, M. J. Hartmann, and R. Fazio, Steady-state phase diagram of a driven QED-cavity array with cross-Kerr nonlinearities, Phys. Rev. A **90**, 023827 (2014).
[42] M. Foss-Feig, P. Niroula, J. T. Young, M. Hafezi, A. V. Gorshkov, R. M. Wilson, and M. F. Maghrebi, Emergent equilibrium in many-body optical bistability, Phys. Rev. A **95**, 043826 (2017).
[43] M. Biondi, G. Blatter, H. E. Türeci, and S. Schmidt, Nonequilibrium gas-liquid transition in the driven-dissipative photonic lattice, Phys. Rev. A **96**, 043809 (2017).
[44] C.-K. Chan, T. E. Lee, and S. Gopalakrishnan, Limit-cycle phase in driven-dissipative spin systems, Phys. Rev. A **91**, 051601(R) (2015).
[45] R. M. Wilson, K. W. Mahmud, A. Hu, A. V. Gorshkov, M. Hafezi, and M. Foss-Feig, Collective phases of strongly interacting cavity photons, Phys. Rev. A **94**, 033801 (2016).
[46] H. Spohn, An algebraic condition for the approach to equilibrium of an open n-level system, Lett. Math. Phys. **2**, 33 (1977).
[47] F. Minganti, A. Biella, N. Bartolo, and C. Ciuti, Spectral theory of Liouvillians for dissipative phase transitions, Phys. Rev. A **98**, 042118 (2018).
[48] H. Weimer, Variational Principle for Steady States of Dissipative Quantum Many-Body Systems, Phys. Rev. Lett. **114**, 040402 (2015).
[49] M. Biondi, S. Lienhard, G. Blatter, H. E. Türeci, and S. Schmidt, Spatial correlations in driven-dissipative photonic lattices, New J. Phys. **19**, 125016 (2017).
[50] J. Jin, A. Biella, O. Viyuela, L. Mazza, J. Keeling, R. Fazio, and D. Rossini, Cluster Mean-Field Approach to the Steady-State Phase Diagram of Dissipative Spin Systems, Phys. Rev. X **6**, 031011 (2016).
[51] A. J. Daley, Quantum trajectories and open many-body quantum systems, Adv. Phys. **63**, 77 (2014).
[52] T. Prosen and M. Žnidarič, Matrix product simulations of non-equilibrium steady states of quantum spin chains, J. Stat. Mech. (**2009**) P02035.
[53] J. J. Mendoza-Arenas, S. R. Clark, S. Felicetti, G. Romero, E. Solano, D. G. Angelakis, and D. Jaksch, Beyond mean-field bistability in driven-dissipative lattices: Bunching-antibunching transition and quantum simulation, Phys. Rev. A **93**, 023821 (2016).
[54] F. Vicentini, F. Minganti, R. Rota, G. Orso, and C. Ciuti, Critical slowing down in driven-dissipative Bose-Hubbard lattices, Phys. Rev. A **97**, 013853 (2018).
[55] J. Jin, A. Biella, O. Viyuela, C. Ciuti, R. Fazio, and D. Rossini, Phase diagram of the dissipative quantum ising model on a square lattice, Phys. Rev. B **98**, 241108(R) (2018).
[56] A. Kshetrimayum, H. Weimer, and R. Orús, A simple tensor network algorithm for two-dimensional steady states, Nat. Commun. **8**, 1291 (2017).
[57] Z. Cai and T. Barthel, Algebraic versus Exponential Decoherence in Dissipative Many-Particle Systems, Phys. Rev. Lett. **111**, 150403 (2013).

[58] K. Macieszczak, M. Guţă, I. Lesanovsky, and J. P. Garrahan, Towards a Theory of Metastability in Open Quantum Dynamics, Phys. Rev. Lett. **116**, 240404 (2016).
[59] See Supplemental Material at http://link.aps.org/supplemental/10.1103/PhysRevLett.124.043601 for additional details about: (i) the relation between bimodality and bistability, (ii) the Ising version of the model in 2D, (iii) MPO simulations in 2D, (iv) the relation between extreme states and bistability, and (v) the MFQF method.
[60] H. Landa, M. Schiró, and G. Misguich, Correlation-induced steady states and limit cycles in driven dissipative quantum systems, arXiv:2001.05474.
[61] E. Mascarenhas, H. Flayac, and V. Savona, Matrix-product-operator approach to the nonequilibrium steady state of driven-dissipative quantum arrays, Phys. Rev. A **92**, 022116 (2015).
[62] U. Schollwöck, The density-matrix renormalization group in the age of matrix product states, Ann. Phys. (Amsterdam) **326**, 96 (2011).
[63] M. P. Zaletel, R. S. K. Mong, C. Karrasch, J. E. Moore, and F. Pollmann, Time-evolving a matrix product state with long-ranged interactions, Phys. Rev. B **91**, 165112 (2015).
[64] G. Benenti, G. Casati, T. Prosen, D. Rossini, and M. Žnidarič, Charge and spin transport in strongly correlated one-dimensional quantum systems driven far from equilibrium, Phys. Rev. B **80**, 035110 (2009).
[65] ITensor Library, http://itensor.org (version 2.1).
[66] K. Bidzhiev and G. Misguich, Out-of-equilibrium dynamics in a quantum impurity model: Numerics for particle transport and entanglement entropy, Phys. Rev. B **96**, 195117 (2017).
[67] E. Stoudenmire and S. R. White, Studying two-dimensional systems with the density matrix renormalization group, Annu. Rev. Condens. Matter Phys. **3**, 111 (2012).
[68] D. C. Rose, K. Macieszczak, I. Lesanovsky, and J. P. Garrahan, Metastability in an open quantum Ising model, Phys. Rev. E **94**, 052132 (2016).
[69] W. Casteels, R. Fazio, and C. Ciuti, Critical dynamical properties of a first-order dissipative phase transition, Phys. Rev. A **95**, 012128 (2017).
[70] D. Porras and J. I. Cirac, Effective Quantum Spin Systems with Trapped Ions, Phys. Rev. Lett. **92**, 207901 (2004).
[71] A. Friedenauer, H. Schmitz, J. T. Glueckert, D. Porras, and T. Schaetz, Simulating a quantum magnet with trapped ions, Nat. Phys. **4**, 757 (2008).
[72] C. Schneider, D. Porras, and T. Schaetz, Experimental quantum simulations of many-body physics with trapped ions, Rep. Prog. Phys. **75**, 024401 (2012).
[73] R. Islam, C. Senko, W. C. Campbell, S. Korenblit, J. Smith, A. Lee, E. E. Edwards, C.-C. J. Wang, J. K. Freericks, and C. Monroe, Emergence and frustration of magnetism with variable-range interactions in a quantum simulator, Science **340**, 583 (2013).
[74] J. Smith, A. Lee, P. Richerme, B. Neyenhuis, P. W. Hess, P. Hauke, M. Heyl, D. A. Huse, and C. Monroe, Many-body localization in a quantum simulator with programmable random disorder, Nat. Phys. **12**, 907 (2016).